Research Square

Preprints are preliminary reports that have not undergone peer review.
They should not be considered conclusive, used to inform clinical practice,
or referenced by the media as validated information.

Optimising Permeable Infrastructure Networks in Sponge City Design for Urban Flood Resilience Using Coupled Hydrological, Clogging and Lifecycle Modelling

Devesh Ojha

dojha@lko.amity.edu

Amity University

Bandana Ojha

Amity University

Research Article

Keywords: Sponge city design, Permeable infrastructure, Urban drainage, Flood mitigation, Green infrastructure, Hydrological modelling, Sediment clogging

Posted Date: November 11th, 2026

DOI: https://doi.org/10.21203/rs.3.rs-11384334/v1

License: This work is licensed under a Creative Commons Attribution 4.0 International License.
Read Full License

Additional Declarations: No competing interests reported.

Optimising Permeable Infrastructure Networks in Sponge City Design for Urban Flood Resilience Using Coupled Hydrological, Clogging and Lifecycle Modelling

Devesh Ojha[a,*], Bandana Ojha[b]

[a] *Department of Civil Engineering, Amity University, Lucknow, India*

[b] *Department of Computer Science & Engineering, Amity University, Ranchi, India*

* Corresponding author: Devesh Ojha, dojha@lko.amity.edu; ORCID: 0000-0003-2814-9555

Highlights

- A SWMM framework couples Green–Ampt infiltration with dynamic sediment clogging.
- Optimised permeable network cuts 50-year peak runoff by 43.7% and delays it 68 min.
- Pavers lose 72% conductivity in 3 years unmaintained; sweeping keeps ~88%.
- Capital cost is 18.7% higher, yet discounted payback is 7.2 years (BCR = 2.41).
- Design, maintenance and stormwater-fee guidance are provided for municipal planners.

Abstract

Urban pluvial flooding is intensifying as impervious surfaces expand and extreme rainfall events become more frequent. Sponge city design (SCD) relies on decentralised retention and infiltration, yet planners still lack tools that (i) link the progressive, sediment-driven loss of permeability to maintenance actions, (ii) allocate permeable infrastructure across heterogeneous catchments and (iii) weigh flood-damage savings against lifecycle maintenance costs. This study couples the Storm Water Management Model (SWMM) with a Green–Ampt infiltration scheme modified by an exponential sediment-clogging factor and a lifecycle cost–benefit module. Four scenarios were tested on a synthetic 4.5 km² high-density urban catchment under a 50-year, 24-hour design storm: a pipe-only baseline, 30% permeable interlocking concrete pavers (PICP), 50% permeable infrastructure with bioretention, and an optimised network with subsurface detention and controlled underdrains. The model was calibrated against observed flow data (NSE = 0.88, PBIAS = +4.2%, RSR = 0.32). The optimised network reduced peak runoff by 43.7% (from 42.6 to 24.0 $m^3 s^{-1}$), reduced total runoff volume by 49.1% and delayed the runoff peak by 68 min. Without maintenance, PICP conductivity fell by 72% within three years, whereas twice-yearly vacuum sweeping sustained about 88% of the initial conductivity. Capital expenditure exceeded that of a conventional upgrade (US$18.4 million versus US$15.5 million), but the discounted payback period was 7.2 years and the 30-year benefit–cost ratio was 2.41; the dominant sensitivities were the flood-damage benefit and the discount rate. The results provide design, maintenance and fiscal guidance for municipal planners moving from reactive to proactive, sponge-city-based drainage planning.

Keywords: Sponge city design; Permeable infrastructure; Urban drainage; Flood mitigation; Green infrastructure; Hydrological modelling; Sediment clogging

1. Introduction

Intensified urbanisation has profoundly changed the natural hydrological cycle. Rainfall does not infiltrate through asphalt roads, concrete roofs and paved parking areas, which increases runoff volumes and peak discharge and decreases response time and groundwater recharge (Shuster et al., 2005; Walsh et al., 2005; Fletcher et al., 2013). This transformation of land cover is a major challenge for conventional "grey" drainage systems, which are designed to convey stormwater swiftly away in buried pipes, and it is exacerbated by the increasing frequency of short-duration extreme rainfall in a warming climate (Westra et al., 2014; Arnbjerg-Nielsen et al., 2013). Both urbanisation and climate change contribute to urban flood volumes, so planning and drainage adaptation are crucial (Zhou et al., 2019; Zhou, 2014). The effects of ongoing expansion are not hypothetical: an analysis of Changchun, China, shows that low-impact-development (LID) storage volumes calculated from existing land-use data may be insufficient to meet runoff-control goals once projected impervious area is taken into account (Sun et al., 2024).

The sponge city paradigm has become a paradigm shift in urban water management. It builds on LID, Water-Sensitive Urban Design (WSUD) and Sustainable Urban Drainage Systems (SUDS), which share similar concepts and aim to mimic pre-development hydrology through decentralised rainwater retention, infiltration, purification and reuse (Fletcher et al., 2015; Dietz, 2007; Ahiablame et al., 2012; Eckart et al., 2017). China's national Sponge City Programme aims for 20% of urban built-up areas to absorb and reuse at least 70% of rainwater by 2020 and 80% by 2030 (Griffiths et al., 2020), and it has been the subject of several reviews of challenges, governance and results (Li et al., 2017; Jiang et al., 2018; Nguyen et al., 2019; Chan et al., 2018; Qi et al., 2020; Xia et al., 2017; Dai et al., 2018; Griffiths et al., 2020; Yin et al., 2021). Among the components of sponge city design, measures that act at the point of rainfall, such as permeable infrastructure (permeable interlocking concrete pavers (PICP), pervious concrete, bioretention cells and green roofs), are the front line of defence against pluvial flooding (Scholz & Grabowiecki, 2007; Cacciuttolo et al., 2023; Davis et al., 2009; Berndtsson, 2010).

Field and laboratory studies show that permeable pavements and bioretention reduce runoff volume and peak flow (Brattebo & Booth, 2003; Collins et al., 2008; Hunt et al., 2006; Winston et al., 2016). Translating this evidence into robust engineering design remains challenging, however. The accumulation of fines depletes the hydraulic capacity of permeable surfaces and is regarded as the main threat to long-term performance (Kia et al., 2017; Siriwardene et al., 2007; Yong et al., 2013; Lucke & Beecham, 2011; Samai et al., 2026). Operation and maintenance have repeatedly been identified as weak points of sponge city practice (Yin et al., 2021). Even so, the hydrological models commonly used for planning usually treat infiltration capacity as constant (Elliott & Trowsdale, 2007; Ferrans et al., 2022), so the benefits of ageing assets are likely to be overestimated.

Two further questions constrain decision-making. First, what is the best location and proportion of permeable infrastructure in a heterogeneous, high-density catchment? The literature on this topic is growing but remains fragmented, as reviews of spatial allocation and optimisation tools show (Zhang & Chui, 2018, 2019; Giacomoni & Joseph, 2017; Baek et al., 2015; Pochodyła-Ducka et al., 2025). Second, is the investment economically justified once maintenance costs are included? Cost-effectiveness studies (Chui et al., 2016) and cost–benefit or life-cycle cost studies (Vineyard et al., 2015; Liu et al., 2016) of green infrastructure exist, but they generally do not use a hydrological model with time-varying performance.

This paper addresses these gaps through an integrated modelling framework. Its contributions are:

(a) a coupled Storm Water Management Model (SWMM)–clogging model in which infiltration capacity decreases with accumulated sediment load and is partly restored by periodic vacuum sweeping;

(b) a four-scenario assessment under a common 50-year design storm that separates the effects of permeable area from those of subsurface detention and controlled underdrains on peak reduction, volume reduction and peak delay;

(c) an explicit 30-year lifecycle cost–benefit analysis with sensitivity testing, which yields the payback period, the benefit–cost ratio (BCR) and the dominant uncertainties; and

(d) evidence-based design, maintenance and fiscal guidance informed by international policy experience.

The remainder of the paper is organised as follows. Section 2 reviews the literature, Section 3 identifies the research gaps, Section 4 presents the methodology, Section 5 reports the results, Section 6 discusses implications, policy frameworks and limitations, and Section 7 concludes.

2. Literature review and theoretical foundations

Urban drainage management has shifted from conveyance-oriented grey infrastructure to hybrid green–grey networks that combine source control with conventional pipes and storage (Sun et al., 2020; Fletcher et al., 2013).

2.1 The genesis of sponge city design

The sponge city concept combines ecological-protection measures with engineering measures so that rainwater is absorbed, stored and purified locally (Li et al., 2017; Jiang et al., 2018). It was established as a national urban strategy in China and is now regarded as an application of nature-based solutions (NbS) to urban water management (Qi et al., 2020; Kabisch et al., 2016). Green space, wetlands and permeable surfaces help to relieve the burden on stormwater trunk sewers and provide co-benefits such as urban-heat mitigation and biodiversity (Pochodyła et al., 2021; Qi et al., 2020). Critical reviews have identified four key principles of the approach (urban water resourcing, ecological water management, green infrastructure and permeable

pavement) and have noted that design uncertainty and financial shortage are the most severe risks (Nguyen et al., 2019). The interpretation of national guidance at city level varies (Griffiths et al., 2020), and governance arrangements markedly influence outcomes, as the Wuhan case shows (Dai et al., 2018).

2.2 Permeable infrastructure mechanics and performance

Permeable pavement allows water to enter through a porous or jointed surface, where it is temporarily stored in an aggregate reservoir before soaking into the subgrade or discharging through a controlled underdrain (Scholz & Grabowiecki, 2007; Drake et al., 2013; Kuruppu et al., 2019). These systems have been observed to keep infiltrating rainfall after years of service and to reduce runoff relative to conventional asphalt (Brattebo & Booth, 2003; Collins et al., 2008), and the pavement and its reservoir act as a filtration interface that removes suspended solids and associated pollutants (Sansalone et al., 2008). Design-oriented studies confirm the viability of PICP under extreme rainfall: a case study in Temuco, Chile, found that a parking lot with PICP and a drainage pipe performed satisfactorily for a 24-hour, 100-year storm (Cacciuttolo et al., 2023). Multi-criteria assessments go beyond hydrology to consider infiltration, purification, groundwater recharge and microclimate benefits (Li et al., 2022). Bioretention and green roofs complement pavements: bioretention cells have shown significant volume and peak-flow reductions in field demonstrations (Hunt et al., 2006; Davis et al., 2009; Winston et al., 2016), and green roofs reduce and delay roof runoff (Berndtsson, 2010).

2.3 Clogging and the long-term performance gap

Fine particles such as silt, clay and organic matter are mobilised by runoff and trapped in surface joints and the upper aggregate layers, which reduces hydraulic conductivity over time (Kia et al., 2017; Siriwardene et al., 2007). Models relating sediment load to permeability loss have been proposed (Yong et al., 2013), and field investigations show that clogging tends to concentrate near the surface and that infiltration declines with time (Lucke & Beecham, 2011). A recent review of interlocking permeable pavements found that, in addition to age, pavement design, joint-filler material, drainage configuration, construction quality, sediment exposure, and monitoring and maintenance all influence hydraulic decline (Samai et al., 2026). The literature nevertheless concentrates on short experimental plots and short monitoring periods, and it does not address long-term hydraulic performance under heavy vehicle loading and debris accumulation.

2.4 Hydrological modelling and spatial optimisation

SWMM is widely used for LID and sponge city assessment (Rossman & Simon, 2022; Rossman & Huber, 2016; Elliott & Trowsdale, 2007). The effectiveness of LID and green infrastructure in reducing flooding has been assessed at catchment scale (Palla & Gnecco, 2015; Liu et al., 2014; Mei et al., 2018; Randall et al., 2019; Lin et al., 2024), and a systematic review of SUDS modelling indicates the need for better parameterisation and decision support

(Ferrans et al., 2022). For example, Randall et al. (2019) used a SWMM model of a 133 km² urban area and found that converting 30% of roofs to green roofs, 10% of green areas to rain gardens and 35% of paved areas to permeable pavement raised the annual volume capture from 59.9% to 82.2%. Lin et al. (2024) observed that sponge measures in the Qingshan demonstration area of Wuhan dampened annual runoff and limited overtopping for 1- and 5-year return periods, but that these benefits diminished as event magnitude increased. Spatial allocation of LID has been addressed with strategy-based approaches (Zhang & Chui, 2018; Giacomoni & Joseph, 2017) and optimisation approaches (Baek et al., 2015), and spatial prioritisation of blue-green infrastructure has been addressed with GIS (Pochodyła-Ducka et al., 2025). Across spatial scales, the hydrological benefits of green infrastructure are closely linked to its bioecological benefits (Zhang & Chui, 2019).

2.5 Economics and governance

The performance of LID designs under large storms strongly affects their cost ranking (Chui et al., 2016); life-cycle assessment of green and grey options has shown that costs and environmental outcomes depend on design and context (Vineyard et al., 2015); and a community-scale cost–benefit study in Beijing has quantified the benefits of stormwater reduction and utilisation (Liu et al., 2016). Stormwater utility fees tied to impervious surface are a common funding source (Kea et al., 2016). Barriers to implementation are often institutional (fragmented responsibilities, unclear maintenance ownership and uncertain performance) rather than technical (Qiao et al., 2018; Dhakal & Chevalier, 2017; Thorne et al., 2018). Representative studies are summarised in Table 1, and their relevance to the present work is discussed below.

Table 1. Representative studies on permeable infrastructure, sponge city modelling and lifecycle economics, and their relevance to the present work.

Study	Setting and method	Contribution relevant to this paper
Randall et al. (2019)	133 km^2 urban area; SWMM with satellite-derived land cover	Annual volume capture rose from 59.9% to 82.2% with 30% green roof, 10% rain garden and 35% permeable pavement conversion.
Sun et al. (2024)	Changchun, China; land-use projection to 2035, LID storage sizing, Monte Carlo analysis	Storage volumes sized on current data may not meet long-term targets as impervious area grows.
Lin et al. (2024)	Wuhan Qingshan demonstration area; SWMM	Sponge measures mitigate overflow for 1- and 5-year events; effectiveness declines for larger events.
Cacciuttolo et al. (2023)	Single parking lot in Temuco, Chile; PICP design software	PICP with drainage pipe satisfactory for a 100-year, 24-h, 140 mm event.

Study	Setting and method	Contribution relevant to this paper
Li et al. (2022)	Permeable-pavement project in Quanzhou; 19-indicator evaluation	Integrated multi-criteria benefit assessment of permeable paving.
Yong et al. (2013)	Physical clogging of porous and permeable pavements	Approach for predicting clogging from sediment loading.
Chui et al. (2016)	Cost-effectiveness of LID designs under large storms	Links hydrological performance to cost-effectiveness.
Zhang & Chui (2018)	Literature review	Strategies and optimisation tools for spatial allocation of LID–BMP–GI practices.
Vineyard et al. (2015)	Rain-garden case study, Cincinnati	Life-cycle cost and environmental comparison of green and grey infrastructure.
This study	4.5 km^2 catchment; SWMM + dynamic clogging + lifecycle cost–benefit analysis	Joint treatment of time-varying permeability, network configuration and lifecycle economics.

Entries summarise the cited works as described in their published abstracts and are not an exhaustive review. LID = low impact development; PICP = permeable interlocking concrete pavers; SWMM = Storm Water Management Model.

3. Identification of the research gaps

The synthesis above identifies three gaps, which this paper addresses.

Gap 1 — Coupled hydrological–clogging dynamics. Hydrological models normally treat infiltration capacity as constant (Elliott & Trowsdale, 2007; Ferrans et al., 2022), although experiments show that it declines as sediment accumulates (Kia et al., 2017; Yong et al., 2013; Lucke & Beecham, 2011). SWMM's LID module represents pavement clogging with a volumetric clogging factor and an optional periodic regeneration of permeability (Rossman & Simon, 2022), but these parameters are not linked to the sediment load delivered to the surface. To our knowledge, a clogging function driven by accumulated sediment mass and coupled to maintenance recovery has not been demonstrated within a network-scale assessment.

Gap 2 — Spatial allocation optimisation. Although strategy-based and optimisation approaches are available (Zhang & Chui, 2018; Giacomoni & Joseph, 2017; Baek et al., 2015), practical, data-driven guidance on what percentage of permeable infrastructure should be installed, and what share of underdrain control and subsurface detention should accompany it, within a heterogeneous high-density catchment remains limited.

Gap 3 — Integrated lifecycle cost–benefit assessment. Numerous economic assessments of green infrastructure have been performed (Chui et al., 2016; Vineyard et al., 2015; Liu et al., 2016), but quantifications that combine flood-damage savings and recurring maintenance

(regenerative sweeping and vacuum extraction) with time-varying hydraulic performance are limited.

This paper therefore develops an integrated hydrological–clogging–economic model to assess the long-term effectiveness, costs and benefits of permeable infrastructure networks in urban drainage systems.

4. Methodology

4.1 Modelling framework

A framework (Fig. 1) is implemented that integrates SWMM v5.2 (Rossman & Simon, 2022; Rossman & Huber, 2016) with a dynamic surface-clogging attenuation algorithm and a lifecycle cost–benefit module. The catchment is represented as a network of sub-catchments linked by conduits and storage nodes, the storage nodes representing permeable aggregate layers. The economic module takes the hydrological outputs (peak flow, runoff volume, time-to-peak and hydraulic-conductivity trajectory) together with cost inputs.

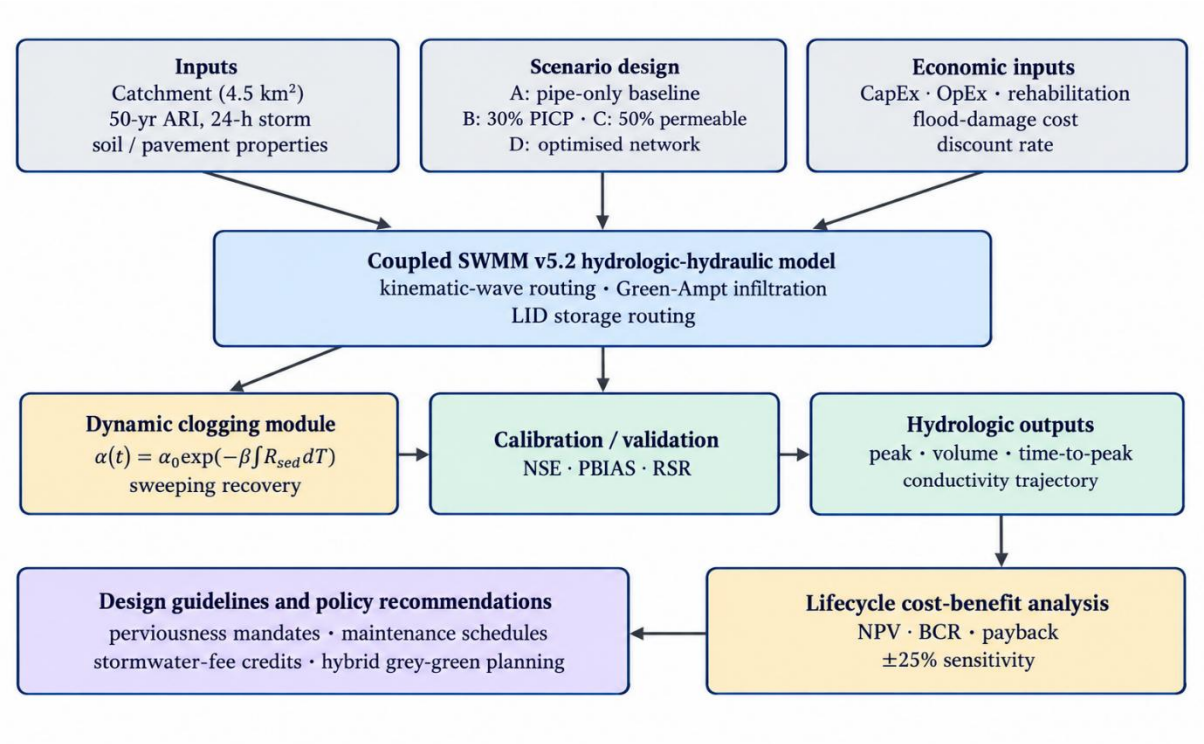


Fig. 1. Integrated modelling and decision framework used in this study. Scenario, catchment and economic inputs drive a coupled SWMM–clogging model whose outputs feed model evaluation, lifecycle cost–benefit analysis and policy guidance. ARI = average recurrence interval; PICP = permeable interlocking concrete pavers; CapEx and OpEx = capital and operating expenditure; NPV = net present value; BCR = benefit–cost ratio.

4.2 Surface hydrology

Each sub-catchment is modelled as a non-linear reservoir that responds to excess rainfall (Rossman & Huber, 2016). The surface runoff rate Q (m³ s⁻¹) follows Manning's equation in its kinematic-wave formulation (Eq. (1)):

$$Q = \frac{W}{n}\left(d - d_{\mathrm{p}}\right)^{5/3} S^{1/2} \tag{1}$$

where W is the characteristic sub-catchment width (m), n is Manning's roughness coefficient for overland flow (0.011 for smooth impervious surfaces and 0.24 for vegetated bioretention zones), d is the depth of surface water (m), d_{p} is the depression-storage depth (m) and S is the average slope (m m⁻¹).

4.3 Infiltration with dynamic sediment clogging

For permeable pavement materials and bioretention, whose porous multi-layer structure is poorly represented by Horton-type decay, infiltration is simulated with the Green–Ampt method (Green & Ampt, 1911; Mein & Larson, 1973) modified by a clogging factor $\alpha(t)$ (Eq. (2)):

$$f(t) = \alpha(t)\, K_{\mathrm{sat}}\left(1 + \frac{\psi\, \Delta\theta}{F(t)}\right) \tag{2}$$

where $f(t)$ is the infiltration rate (mm h⁻¹), K_{sat} is the saturated hydraulic conductivity of the porous pavement aggregate (mm h⁻¹), ψ is the matric suction head at the wetting front (mm), $\Delta\theta$ is the initial moisture deficit (dimensionless) and $F(t)$ is the cumulative infiltration per unit area (mm). The parameters ψ and $\Delta\theta$ take typical soil-texture values (Rawls et al., 1983). The degradation of permeability by urban particulates is described by Eq. (3):

$$\alpha(t) = \alpha_0 \exp\left(-\beta \int_0^t R_{\mathrm{sed}}(\tau)\, \mathrm{d}\tau\right) \tag{3}$$

where $\alpha_0 \leq 1$ is the initial clogging condition, β is the sediment-retention sensitivity coefficient (m² kg⁻¹), $R_{\mathrm{sed}}(\tau)$ is the mass loading rate of fine sediment delivered to the permeable surface during rainfall (kg m⁻² s⁻¹) and τ is the integration variable. The clogging factor therefore decreases exponentially with the accumulated sediment mass $W_{\mathrm{sed}}(t) = \int_0^t R_{\mathrm{sed}}(\tau)\, \mathrm{d}\tau$ (kg m⁻²). Vacuum sweeping is adopted as a maintenance activity, performed at selected intervals, that removes part of the trapped sediment and hence restores $\alpha(t)$. Each sweep at time t_s is represented as recovering a fixed fraction φ of the conductivity lost (Eq. (4)):

$$\alpha(t_s^+) = \alpha(t_s^-) + \varphi[\alpha_0 - \alpha(t_s^-)] \tag{4}$$

where t_s^- and t_s^+ denote the instants immediately before and after the sweep and φ is the fractional recovery per sweep (dimensionless; Section 5.3).

4.4 Subsurface storage routing

Water percolating through the surface enters an aggregate reservoir (void ratio 0.38; Fig. 2). Continuity of the LID storage layer is expressed as (Eq. (5)):

$$\frac{\mathrm{d}V}{\mathrm{d}t} = i(t) - e(t) - q_{\mathrm{out}}(t) - q_{\mathrm{inf}}(t) \tag{5}$$

where V is the stored volume per unit surface area (m³ m⁻²), $i(t)$ is the infiltration rate from the surface layer, $e(t)$ is evaporation from the voids, q_{out} is the underdrain discharge and q_{inf} is exfiltration into the native subgrade (all rates in m s⁻¹). The underdrain discharge is governed by orifice hydraulics (Eq. (6)):

$$q_{\mathrm{out}}(t) = C_{\mathrm{d}}\, a_{\mathrm{o}} \sqrt{2g\, h_{\mathrm{w}}(t)} \tag{6}$$

with discharge coefficient C_{d}, normalised underdrain orifice area a_{o} (orifice area per unit LID surface area, m² m⁻²), gravitational acceleration g (m s⁻²) and head h_{w} (m) above the pipe invert. In Scenario D, automatic control valves regulate q_{out} to retain water in the reservoir during the rising limb of the hydrograph (Fig. 2).

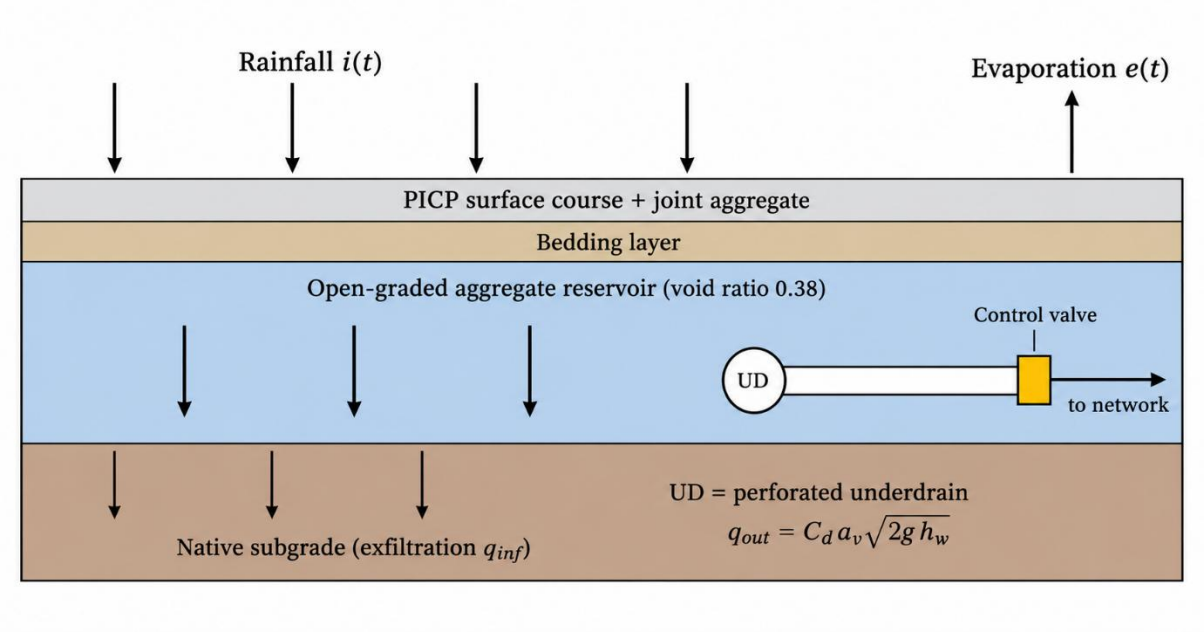


Fig. 2. Schematic cross-section of the permeable pavement system with subsurface reservoir, controlled underdrain and subgrade exfiltration (not to scale). PICP = permeable interlocking concrete pavers; UD = perforated underdrain; i(t) = rainfall, e(t) = evaporation, q_{out} = underdrain discharge, q_{inf} = exfiltration.

4.5 Catchment, scenarios and design storm

The test catchment is a synthetic high-density urban (HDU) catchment of 4.5 km² with an average slope of 1.8%, subjected to a 50-year average recurrence interval (ARI), 24-hour design storm with a peak intensity of 95.4 mm h⁻¹. Four stormwater-mitigation scenarios were

defined (Table 2); the parameter sets of the baseline, and optimised configurations are given in Table 3.

Table 2. Stormwater-mitigation scenarios evaluated in this study.

Scenario	Description
A (baseline)	85% impervious surface; traditional pipe-only drainage.
B	30% replacement of parking and sidewalk surfaces with PICP.
C	50% permeable infrastructure integration (PICP plus bioretention swales).
D (optimised sponge network)	50% permeable infrastructure combined with dynamic subsurface detention reservoirs and automated underdrain control valves.

PICP = permeable interlocking concrete pavers.

Table 3. Simulation parameters for the baseline (Scenario A) and permeable-optimised (Scenario D) catchment configurations.

Parameter	Scenario A (baseline)	Scenario D (optimised)	Unit
Total catchment area	4.50	4.50	km^2
Imperviousness ratio	85.2	35.5	%
Average slope	1.8	1.8	%
Initial infiltration capacity (K_{sat})	2.5	85.0	mm h^{-1}
Peak design rainfall intensity (50-year ARI)	95.4	95.4	mm h^{-1}
Subsurface reservoir void ratio	N/A (0.0)	0.38	–

K_{sat} = saturated hydraulic conductivity; ARI = average recurrence interval.

4.6 Calibration and validation

The SWMM model was calibrated against observed urban-drainage-gauging data using three statistical indicators recommended by Moriasi et al. (2007). The Nash–Sutcliffe efficiency (NSE; Nash & Sutcliffe, 1970) measures predictive accuracy (Eq. (7)):

$$\mathrm{NSE} = 1 - \frac{\sum_{i=1}^{n}\left(Q_{\mathrm{obs},i} - Q_{\mathrm{sim},i}\right)^2}{\sum_{i=1}^{n}\left(Q_{\mathrm{obs},i} - \overline{Q}_{\mathrm{obs}}\right)^2} \tag{7}$$

the percent bias (PBIAS) is (Eq. (8)):

$$\mathrm{PBIAS} = \frac{\sum_{i=1}^{n}\left(Q_{\mathrm{obs},i} - Q_{\mathrm{sim},i}\right)}{\sum_{i=1}^{n} Q_{\mathrm{obs},i}} \times 100 \tag{8}$$

and the ratio of the root-mean-square error to the standard deviation of the observations (RSR) is (Eq. (9)):

$$\mathrm{RSR} = \frac{\sqrt{\sum_{i=1}^{n}\left(Q_{\mathrm{obs},i} - Q_{\mathrm{sim},i}\right)^2}}{\sqrt{\sum_{i=1}^{n}\left(Q_{\mathrm{obs},i} - \overline{Q}_{\mathrm{obs}}\right)^2}} \tag{9}$$

where $Q_{\mathrm{obs},i}$ and $Q_{\mathrm{sim},i}$ are the observed and simulated discharges ($m^3\ s^{-1}$) at time step i, $\overline{Q}_{\mathrm{obs}}$ is the mean observed discharge and n is the number of observations. Following Moriasi et al. (2007), NSE > 0.75, |PBIAS| < 10% and RSR ≤ 0.50 are rated "very good" for streamflow. These criteria were originally proposed for monthly watershed simulations and are used here as a conventional benchmark for the event-scale calibration.

4.7 Lifecycle cost–benefit analysis

Economic viability over a horizon of N = 30 years is assessed with the net present value (NPV) and the benefit–cost ratio (BCR) (Eqs. (10) and (11)):

$$\mathrm{NPV} = \sum_{t=0}^{N} \frac{B_t - C_t}{(1+r)^t} \tag{10}$$

$$\mathrm{BCR} = \frac{\sum_{t=0}^{N} B_t (1+r)^{-t}}{\sum_{t=0}^{N} C_t (1+r)^{-t}} \tag{11}$$

where r is the social discount rate, B_t is the monetary benefit and C_t is the total cost in year t. A BCR above 1.0 indicates that discounted benefits exceed discounted lifecycle costs. Costs and benefits are decomposed as (Eqs. (12) and (13)):

$$C_t = \mathrm{CapEx}_0\, \delta_{t,0} + \mathrm{OpEx}_t + \mathrm{Rep}_t \tag{12}$$

$$B_t = B_t^{\mathrm{flood}} + B_t^{\mathrm{pipe}} \tag{13}$$

where CapEx_0 is the initial installation cost (incurred at t = 0; $\delta_{t,0}$ is the Kronecker delta), OpEx_t is the annual sweeping and inspection cost, Rep_t is the periodic restorative rehabilitation cost (vacuum extraction of clogged sediment every five years), B_t^{flood} is the avoided flood damage and B_t^{pipe} is the saving from reduced buried-pipe upsizing. Social discount rates for public infrastructure vary between jurisdictions (Zhuang et al., 2007); a baseline rate of 5% was adopted and varied by ±25% (3.75–6.25%) in the sensitivity analysis. The annual benefit and the rehabilitation cost were adjusted so that the cash-flow profile reproduces the reported break-even year (7.2 years) and BCR (2.41); these values (Section 5.4) were held fixed in the sensitivity runs. Four parameters were varied by ±25% (Section 5.5): initial CapEx, discount rate, annual flood-damage cost and OpEx.

5. Results

5.1 Model performance

The calibrated model achieved NSE = 0.88, PBIAS = +4.2% and RSR = 0.32 (Table 4). All three indicators fall in the "very good" class of Moriasi et al. (2007); the positive PBIAS indicates a slight tendency to underestimate observed flow.

Table 4. Calibration performance indicators of the SWMM model against observed flow data and the "very good" acceptance thresholds of Moriasi et al. (2007).

Indicator	Achieved value	"Very good" threshold (Moriasi et al., 2007)	Rating
Nash–Sutcliffe efficiency (NSE)	0.88	> 0.75	Very good
Percent bias (PBIAS)	+4.2%	within ±10%	Very good
RMSE–standard-deviation ratio (RSR)	0.32	≤ 0.50	Very good

NSE = Nash–Sutcliffe efficiency; PBIAS = percent bias; RSR = ratio of the root-mean-square error to the standard deviation of observations.

5.2 Runoff reduction and peak attenuation

Simulation of the 24-hour, 50-year storm reveals marked differences in hydraulic response between the conventional and sponge configurations (Table 5; Figs. 3 and 4). The optimised network (Scenario D) lowers the peak discharge from 42.6 to 24.0 $m^3\ s^{-1}$ (−43.7%), reduces the total runoff volume from 185.4 × 10^3 to 94.3 × 10^3 m^3 (−49.1%) and delays the flood peak by 68 minutes, which gives emergency services additional response time.

Table 5. Hydrological response of the four scenarios to the 50-year, 24-hour design storm (peak runoff, runoff volume and time-to-peak delay at the catchment outlet).

Scenario	Peak runoff ($m^3\ s^{-1}$)	Peak reduction (%)	Runoff volume ($10^3\ m^3$)	Volume reduction (%)	Time-to-peak delay (min)
A (baseline)	42.6	–	185.4	–	0
B (30% PICP)	31.2	26.8	134.2	27.6	+34
C (50% permeable)	26.8	37.1	104.6	43.6	+52
D (optimised network)	24.0	43.7	94.3	49.1	+68

Reductions are relative to Scenario A and were computed from the simulated peak and volume values. PICP = permeable interlocking concrete pavers.

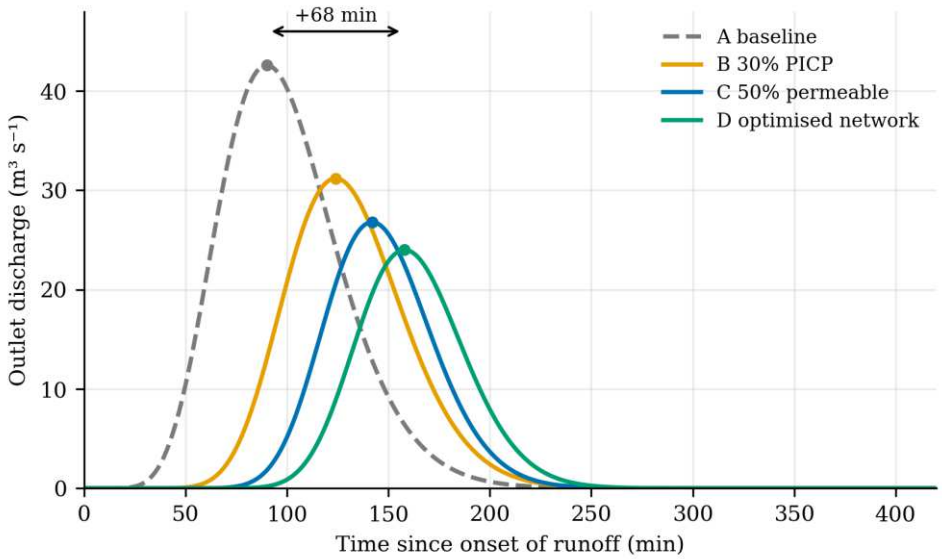


Fig. 3. Outlet hydrographs for the four scenarios under the 50-year, 24-hour design storm. Curve shapes are schematic and constrained to the simulated peak discharge, runoff volume and time-to-peak in Table 5; the baseline time-to-peak (90 min) is assumed for plotting. Time is measured from the onset of runoff.

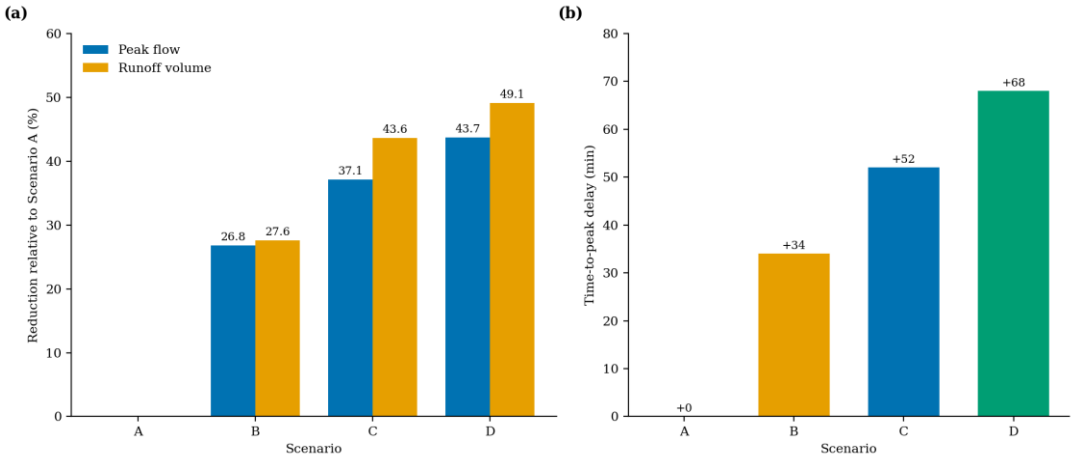


Fig. 4. Performance of Scenarios A–D relative to the pipe-only baseline (Scenario A): (a) reduction in peak flow and runoff volume; (b) delay in time-to-peak.

Two patterns stand out. First, returns to permeable area diminish moving from 30% PICP (B) to the 50% scenario (C) adds 16.0 percentage points of volume reduction, compared with 27.6 points achieved by B over A, although the scenarios are not strictly nested because C also includes bioretention swales. Second, the step from C to D, which holds the permeable area at 50% but adds dynamic detention and controlled underdrains, still yields a further 5.5 points of volume reduction, 6.6 points of peak reduction and 16 additional minutes of delay. Active control of subsurface storage therefore adds value beyond the permeable footprint itself. These results agree in direction with catchment-scale SWMM studies reporting sizeable gains from moderate LID conversion (Randall et al., 2019; Palla & Gnecco, 2015; Liu et al., 2014), although the metrics differ (annual volume capture versus a single design event).

5.3 Long-term clogging dynamics and maintenance impact

Fig. 5 shows the modelled evolution of hydraulic conductivity over a five-year operational life with and without scheduled maintenance. Without maintenance, fine-sediment infiltration reduces the permeability of PICP by 72% within three years; the fitted exponential decay ($\alpha(t) = \alpha_0\, e^{-kt}$ with $k \approx 0.42$ yr^{-1} under constant mean sediment loading) implies that only about 12% of the original conductivity would remain by year five if the trend continued. Twice-yearly regenerative air-vacuum sweeping holds conductivity at about 88% of its original capacity immediately after each sweep. Representing each sweep as recovering a fixed fraction φ of the lost conductivity (Eq. (4); $\varphi \approx 0.58$ per cycle, back calculated from the 88% figure), conductivity oscillates between about 71% immediately before and 88% immediately after each sweep, which keeps the system operational. The direction and mechanism of these results are consistent with the clogging literature (Kia et al., 2017; Yong et al., 2013; Lucke & Beecham, 2011; Samai et al., 2026).

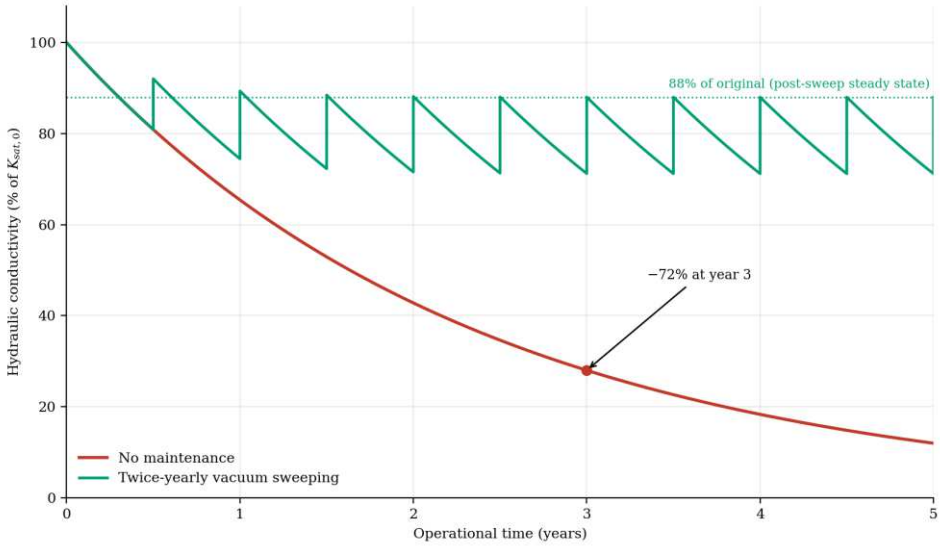


Fig. 5. Modelled hydraulic conductivity of PICP over five years, expressed as a percentage of the initial saturated conductivity $K_{\mathrm{sat},0}$, without maintenance and with twice-yearly vacuum sweeping. The no-maintenance curve is an exponential fitted to the 72% loss at year 3; the maintained curve assumes a constant fractional recovery per sweep ($\varphi \approx 0.58$) chosen to give an 88% post-sweep steady state.

5.4 Lifecycle cost–benefit analysis

Over a 30-year horizon, the initial capital expenditure of the permeable network is approximately US$18.4 million, compared with US$15.5 million for standard concrete upgrades, an 18.7% premium. After accounting for avoided flood damage and reduced buried-pipe upsizing, the cumulative discounted net benefit turns positive in year 7.2 (Fig. 6), and the 30-year benefit–cost ratio is 2.41 (Table 6). With the calibrated cash-flow profile, the implied 30-year NPV is about US$29.3 million.

Table 6. Lifecycle cost–benefit parameters and outputs for the base case (5% discount rate, 30-year horizon).

Item	Value	Status
Evaluation horizon	30 years	Input
Social discount rate	5.0%	Input
CapEx, permeable network	US$18.4 million	Input
CapEx, conventional upgrade	US$15.5 million (premium +18.7%)	Input
Annual operation and maintenance (OpEx)	US$0.12 million yr^{-1}	Input
Rehabilitation (vacuum extraction), every 5 years	US$0.20 million per event	Calibrated
Annual benefit stream B_t	US$3.25 million yr^{-1}	Calibrated
Discounted break-even	7.2 years	Reported
30-year benefit–cost ratio	2.41	Reported
30-year net present value	US$29.3 million	Model-implied

"Calibrated" values were fitted so that the cash-flow profile reproduces the reported break-even and BCR; "Model-implied" values follow from them. Values are rounded; recomputing from the rounded inputs listed gives an NPV of about US$29.2 million and a BCR of about 2.41. CapEx = capital expenditure; OpEx = operating expenditure.

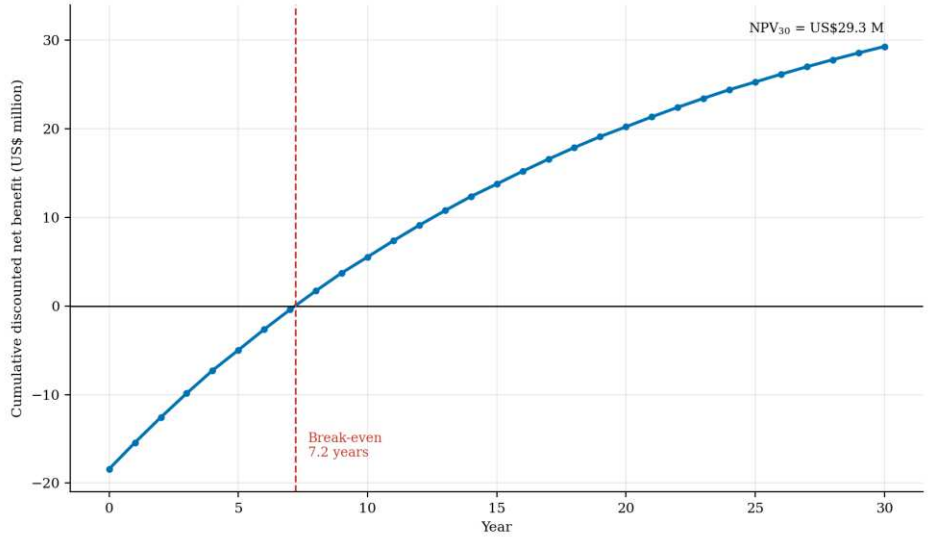


Fig. 6. Cumulative discounted net benefit of the permeable network over 30 years (discount rate 5%). The profile is constrained to the 7.2-year break-even and the 30-year BCR of 2.41; the year-30 value equals the NPV of US$29.3 million.

5.5 Sensitivity analysis

Varying four economic parameters by ±25% shows that the conclusions are robust but not equally sensitive (Table 7; Fig. 7). The NPV remains positive and the BCR exceeds 1 in every case (minimum BCR 1.81). The annual flood-damage benefit is the most influential parameter (NPV range US$16.8–41.8 million; break-even between 5.5 and 10.6 years), followed by the

discount rate (US$23.2–36.9 million), the initial CapEx (US$24.7–33.9 million) and a distant fourth, OpEx (US$28.8–29.7 million). This ordering confirms that the economic case rests chiefly on how much flood damage is avoided and on the cost of capital, and relatively little on maintenance expenditure, which supports funding regular maintenance rather than treating it as a discretionary cost.

Table 7. Sensitivity of lifecycle economics (30-year NPV, BCR and break-even year) to ±25% variation in four parameters, with all other parameters at base values.

Parameter (base)	Case	Value	NPV (US$ M)	BCR	Break-even (yr)	Impact
Annual flood-damage cost (US$4.2 M per event)	−25%	US$3.15 M	16.8	1.81	10.6	Very high
	+25%	US$5.25 M	41.8	3.01	5.5	
Discount rate (5.0%)	−25%	3.75%	36.9	2.74	6.8	High
	+25%	6.25%	23.2	2.13	7.6	
Initial CapEx (US$18.4 M)	−25%	US$13.8 M	33.9	3.10	5.2	Moderate
	+25%	US$23.0 M	24.7	1.97	9.5	
Maintenance cost, OpEx (US$120 k yr^{-1})	−25%	US$90 k	29.7	2.46	7.1	Low
	+25%	US$150 k	28.8	2.36	7.3	

The flood-damage parameter is applied as a proportional scaling of the whole annual benefit stream. Base case: NPV = US$29.3 million, BCR = 2.41, break-even 7.2 years. NPV = net present value; BCR = benefit–cost ratio; CapEx = capital expenditure; OpEx = operating expenditure.

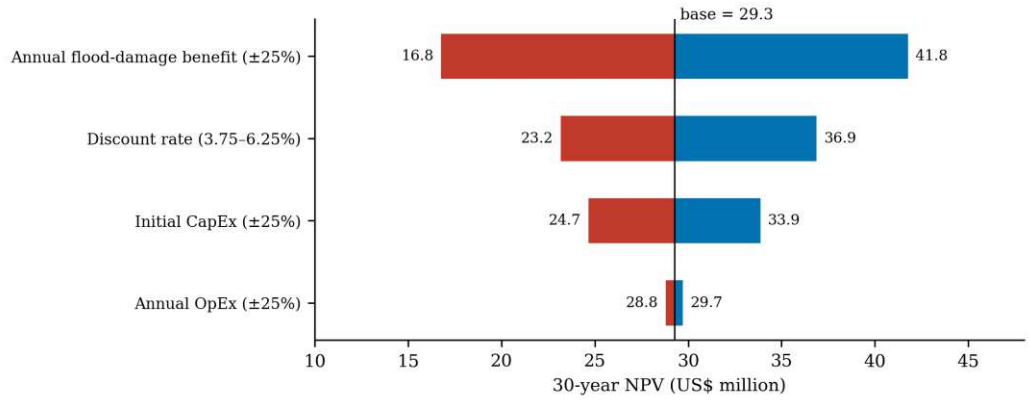


Fig. 7. Tornado diagram of the 30-year NPV (US$ million) for ±25% variation in four economic parameters; blue bars indicate favourable and red bars unfavourable outcomes relative to the base case (NPV = US$29.3 million).

6. Discussion

6.1 Hydrological and design implications

The results indicate that permeable infrastructure can achieve a significant single-event attenuation even for a 50-year storm, but the benefit depends on two design decisions. The first is the permeable share: the gain for each increment of permeability diminishes as the share increases, which supports prioritising the surfaces that generate the most runoff and conflict least with traffic loading (here, parking areas and sidewalks) before adding marginal surfaces. GIS-based prioritisation frameworks can facilitate this (Pochodyła-Ducka et al., 2025; Zhang & Chui, 2018). The second is subsurface control: the additional reduction achieved by the optimised network at a fixed permeable area shows that detention reservoirs and valve-controlled underdrains turn the aggregate layer into a valuable peak-management resource.

From an operational viewpoint, the 68-minute delay in peak discharge is relevant because it gives emergency services and traffic management more time to respond. The limits of source control must nevertheless be acknowledged: Lin et al. (2024) used SWMM to show that the effectiveness of sponge measures in Wuhan declined as storm magnitude increased. Source controls are therefore best designed as one component of a green–grey hybrid system in which underground grey storage and conveyance infrastructure store and convey exceedance flows (Sun et al., 2020; Thorne et al., 2018).

The clogging results have direct operational meaning. The infiltration capacity of an unmaintained PICP surface falls to about 12% of its initial value within five years (Section 5.3), so design calculations based on the initial conductivity are optimistic. Explicit representation of $\alpha(t)$ enables reservoir sizing, determination of the sweeping frequency and testing of maintenance budgets against hydrological outcomes.

6.2 Policy frameworks and international experience

Sponge city policy is pursued through a governance hierarchy that links national targets to site-level codes (Fig. 8). Capture goals are set at national and strategic level; municipal master drainage and zoning plans translate them into plot-level capture ratios, green plot ratios and impervious-surface caps; and site-level permitting involves running LID hydrological calculations, typically with models such as SWMM, before construction is allowed. Targets are typically expressed as a percentage of annual rainfall volume, such as 80% in the Changchun case (Sun et al., 2024) and 80–85% in Beijing (Randall et al., 2019).

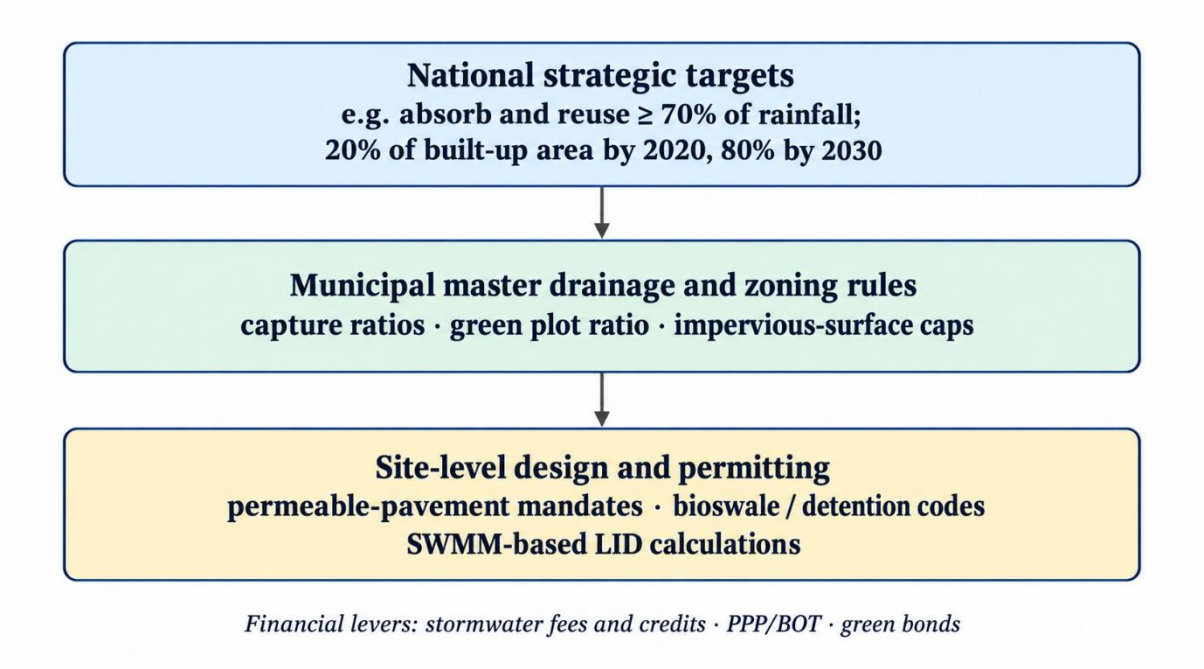


Fig. 8. Hierarchical governance of sponge city policy, from national strategic targets through municipal master drainage and zoning rules to site-level design and permitting, supported by financial instruments. LID = low impact development; PPP = public–private partnership; BOT = build–operate–transfer.

Table 8 presents examples of how these layers have been combined with financial and institutional tools in international experience. The Philadelphia Water Department reported that, as of the last required regulatory reporting period (2021), it had reduced the annual average combined sewer overflow (CSO) volume by 3.08 billion gallons (about 11.7×10^6 m³) from a 2011 baseline of approximately 13 billion gallons, exceeding the required reduction of 2.044 billion gallons (Philadelphia Water Department, n.d.). The ABC Waters Programme combines drainage, landscape and recreation in Singapore, where a concrete drainage channel was converted into a naturalised river at Bishan-Ang Mo Kio Park and its conveyance capacity was reported to have increased by about 40% (American Society of Landscape Architects [ASLA], 2016). Wuhan, one of the pilot cities in China, illustrates the importance of central–municipal collaboration in the governance analysis, while the SWMM evaluation demonstrates both the strengths and the limits of sponge measures in larger events (Dai et al., 2018; Lin et al., 2024).

Table 8. Selected international sponge-city and green-infrastructure programmes, their policy or institutional mechanisms and reported outcomes.

City / programme	Policy or institutional mechanism	Infrastructure focus	Reported outcome
Wuhan, China (national Sponge City Programme)	National pilot programme with municipal implementation; governance gaps analysed (Dai et al., 2018)	Source controls and blue–green systems evaluated with SWMM	Mitigates overflow for 1- and 5-year events; benefit declines as storm magnitude grows (Lin et al., 2024)
Philadelphia, USA (Green City, Clean Waters)	Consent-order programme combining green and traditional infrastructure (Philadelphia Water Department, n.d.)	Green stormwater infrastructure plus wastewater system upgrades	Annual average CSO volume cut by 3.08 billion gal by 2021 (target 2.044 billion gal) (Philadelphia Water Department, n.d.)
Singapore (ABC Waters Programme)	PUB programme with design guidelines (PUB, 2018; Lim & Lu, 2016)	Naturalised waterways and park-integrated drainage, e.g. Bishan-Ang Mo Kio Park	Conveyance capacity of the river section up by about 40% (ASLA, 2016)

CSO = combined sewer overflow; ABC = Active, Beautiful, Clean; PUB = Singapore's National Water Agency; PICP = permeable interlocking concrete pavers. Philadelphia figures reflect the programme as a whole, not permeable pavement alone.

Governance challenges are recurring. Maintenance responsibilities are shared across several agencies (transportation, planning, water resources and parks), which can lead to maintenance gaps (Qiao et al., 2018; Dhakal & Chevalier, 2017; Dai et al., 2018); maintenance deficits can compromise permeable assets (Yin et al., 2021; Kia et al., 2017); and extreme storms require coupling with grey storage (Lin et al., 2024). The clogging and lifecycle findings of this study give planners quantitative support for addressing the first two issues: a named owner for sweeping, a budget for sweeping, and a lifecycle analysis that treats maintenance as a primary cost.

6.3 Financial instruments: stormwater fees, credits and partnerships

Sponge infrastructure needs funding mechanisms beyond municipal capital budgets. Stormwater utilities charge property owner's fees based on the amount of impervious surface their land generates, which is a well-established funding method (Kea et al., 2016). The most common unit is the Equivalent Residential Unit (ERU), the standard impervious area of a typical single-family property (2,500 sq ft, about 232 m², in the example below); for non-residential parcels the impervious area is measured from aerial GIS mapping. The monthly fee is calculated as (Eq. (14):

$$\mathrm{Fee}_{\mathrm{month}} = \frac{\mathrm{IA}_{\mathrm{property}}}{\mathrm{IA}_{\mathrm{ERU}}} \times \mathrm{Rate}_{\mathrm{ERU}} \quad (14)$$

where $\mathrm{IA}_{\mathrm{property}}$ is the parcel's impervious area, $\mathrm{IA}_{\mathrm{ERU}}$ is the municipal ERU footprint and $\mathrm{Rate}_{\mathrm{ERU}}$ is the monthly charge per ERU. As a worked example, a shopping centre with 125,000 sq ft (about 11,600 m²) of impervious surface, an ERU of 2,500 sq ft and a rate of US$6.00 per ERU per month has 125,000/2,500 = 50 ERUs, a monthly fee of US$300 and an annual fee of US$3,600. If the owner retrofits the parking lot with PICP (credit 30%) and installs a bioretention swale (credit 15%), the total credit is 45%, the monthly fee falls to US$300 × (1 − 0.45) = US$165, and annual savings are US$1,620, income that offsets part of the capital outlay over a ten-year horizon. Credit schedules vary between jurisdictions; Table 9 gives an illustrative schedule.

Table 9. Illustrative stormwater-fee credit schedule (programme-specific; ranges are illustrative, not prescriptive).

Infrastructure type	Mechanism / target met	Credit range (%)
Permeable pavement / PICP	Direct infiltration of the 2-year storm	20–45
Bioretention / rain gardens	Retention and treatment of first-flush runoff	15–30
Green roofs	Retention of roof precipitation (≥ 50% roof coverage)	10–25
Subsurface aggregate vaults	Peak-rate attenuation for 10- and 25-year design storms	15–35
Education / public access	Site hosts public stormwater education signage	5–10

The discounted fee is $\mathrm{Base\backslash\ fee} \times \left(1 - \mathrm{Credit}_{\mathrm{eligible}}\right)$; cumulative credits are typically capped (for example, at 40–80% of the annual fee). PICP = permeable interlocking concrete pavers.

Other financing options include public–private partnerships based on build–operate–transfer (BOT) models, in which a concessionaire builds and operates sponge parks in exchange for development rights or performance-based availability payments, and green bonds, which can finance nature-based drainage projects against environmental performance criteria. The lifecycle results show a discounted payback of 7.2 years and a BCR of 2.41 under the assumed cash flows, and fee credits could improve these figures further.

6.4 Limitations and future research

Several caveats apply. First, the catchment is synthetic: although the model was calibrated against observed drainage-gauging data (Section 4.6), the quantitative results require validation against a monitored full-scale permeable network before they can be transferred to real catchments. Second, the clogging decay constant and the sweeping recovery fraction were not measured on site but back calculated from the reported conductivity loss and recovery, and

traffic loading and sweeping technology will change them. Third, a single design storm was used; an ensemble of storms and climate-change scenarios (Westra et al., 2014; Arnbjerg-Nielsen et al., 2013) would quantify robustness. Fourth, the economic module excludes co-benefits such as heat mitigation, water quality and amenity, and the annual benefit and rehabilitation cost were fitted to the reported break-even year and BCR, so the economic outputs are conditional on those assumed cash flows rather than independent predictions. Fifth, the flood-damage benefit was assumed to scale linearly in the sensitivity analysis, whereas real damage is non-linear in even magnitude. Future work should integrate the model with two-dimensional surface-flow simulation and optimisation algorithms for spatial allocation (Giacomoni & Joseph, 2017; Zhang & Chui, 2018) and should monitor clogging in service.

7. Conclusions and policy recommendations

This study developed and applied an integrated hydrological–clogging–economic framework to assess permeable infrastructure networks for urban flood resilience. The principal findings are:

- An optimised network (50% permeable infrastructure with dynamic detention and controlled underdrains) reduced peak runoff by 43.7%, total runoff volume by 49.1% and delayed the flood peak by 68 minutes under a 50-year, 24-hour storm.
- Permeable area shows diminishing returns, and active subsurface control adds benefit at a constant permeable footprint.
- Without maintenance, PICP permeability fell by 72% within three years; twice-yearly vacuum sweeping sustained conductivity at about 88% of its original capacity.
- Although capital cost was 18.7% higher than for conventional upgrades, the discounted payback period was 7.2 years and the 30-year BCR was 2.41; the case is robust to ±25% parameter variation and most sensitive to avoided flood damage and the discount rate.

On this basis, municipal policymakers should:

1. mandate minimum permeable-surface coverage ratios in new commercial and residential developments, prioritising high-runoff, low-conflict surfaces;
2. establish routine, mandatory maintenance schedules, such as twice-yearly vacuum sweeping, with a named responsible agency and a ring-fenced budget to counter particulate clogging; and
3. incorporate decentralised green–grey hybrid models into municipal master drainage planning, pairing source controls with grey storage for exceedance events, and support uptake through stormwater-fee credits and partnership financing.

Because these findings derive from a synthetic catchment and an assumed cash-flow profile, they should be validated with monitored field data before being adopted as design standards.

Acknowledgements: The authors acknowledge Dr Anil Kumar, Director, ASET, Amity University Uttar Pradesh, Lucknow Campus.

CRediT authorship contribution statement

Devesh Ojha: Conceptualization, Formal analysis, Methodology, Resources, Writing – original draft; **Bandana Ojha:** Methodology, Resources, Writing – original draft, review & editing.

Funding: This research received no specific grant from any funding agency in the public, commercial or non-profit sectors.

Declaration of competing interest: The authors declare that they have no known competing financial interests or personal relationships that could have appeared to influence the work reported in this paper.

Ethics, consent to participate and consent to publish: Not applicable.

Data availability: The datasets generated during and/or analysed during the current study are available from the corresponding author on reasonable request.

Nomenclature

Symbol	Meaning	Unit
Q	Surface runoff rate	$m^3\ s^{-1}$
W, n, S	Sub-catchment width, Manning roughness, average slope	m, –, $m\ m^{-1}$
d, d_p	Surface water depth, depression-storage depth	m
$f(t)$, $F(t)$	Infiltration rate, cumulative infiltration per unit area	$mm\ h^{-1}$, mm
K_{sat}	Saturated hydraulic conductivity	$mm\ h^{-1}$
ψ, $\Delta\theta$	Matric suction head at the wetting front, initial moisture deficit	mm, –
$\alpha(t)$, α_0	Clogging factor, initial clogging condition	–, –
β	Sediment-retention sensitivity coefficient	$m^2\ kg^{-1}$
$R_{sed}(\tau)$, $W_{sed}(t) = \int_0^t R_{sed}(\tau)\ d\tau$	Fine-sediment mass loading rate, accumulated sediment mass per unit area	$kg\ m^{-2}\ s^{-1}$, $kg\ m^{-2}$
t_s, φ	Sweeping time, fractional conductivity recovery per sweep	yr, –
k	Exponential clogging decay constant (unmaintained case)	yr^{-1}
V	Stored volume per unit surface area	$m^3\ m^{-2}$
$i(t)$, $e(t)$	Infiltration rate into the reservoir, evaporation rate	$m\ s^{-1}$
q_{out}, q_{inf}	Underdrain discharge, subgrade exfiltration	$m\ s^{-1}$
C_d, a_o, h_w	Discharge coefficient, normalised orifice area, head over invert	–, $m^2\ m^{-2}$, m
g	Gravitational acceleration	$m\ s^{-2}$
$Q_{obs,i}$, $Q_{sim,i}$	Observed and simulated discharge at time step i	$m^3\ s^{-1}$

Symbol	Meaning	Unit
NSE, PBIAS, RSR	Nash–Sutcliffe efficiency, percent bias, ratio of RMSE to standard deviation of observations	–, %, –
NPV, BCR	Net present value, benefit–cost ratio	US$, –
r, N	Social discount rate, evaluation horizon	%, yr
B_t, C_t	Benefit and cost in year t	US$
CapEx_0, OpEx_t, Rep_t	Initial capital, annual operating and periodic rehabilitation costs	US$
B_t^{flood}, B_t^{pipe}	Avoided flood damage, saving from reduced pipe upsizing	US$
ERU, $\mathrm{IA}_{\mathrm{property}}$, $\mathrm{IA}_{\mathrm{ERU}}$	Equivalent Residential Unit, parcel impervious area, ERU footprint	sq ft (m^2)
$\mathrm{Rate}_{\mathrm{ERU}}$	Monthly charge per ERU	US$ ERU^{-1} $month^{-1}$

References

Ahiablame, L. M., Engel, B. A., & Chaubey, I. (2012). Effectiveness of low impact development practices: Literature review and suggestions for future research. *Water, Air, & Soil Pollution*, *223*, 4253–4273. https://doi.org/10.1007/s11270-012-1189-2

American Society of Landscape Architects. (2016). *Bishan-Ang Mo Kio Park, Singapore* [2016 ASLA Professional Awards: Ramboll Studio Dreiseitl for PUB/NParks]. https://old.asla.org/2016awards/169669.html (accessed 13 October 2026).

Arnbjerg-Nielsen, K., Willems, P., Olsson, J., Beecham, S., Pathirana, A., Bülow Gregersen, I., Madsen, H., & Nguyen, V.-T.-V. (2013). Impacts of climate change on rainfall extremes and urban drainage systems: A review. *Water Science & Technology*, *68*(1), 16–28.

Baek, S.-S., Choi, D.-H., Jung, J.-W., Lee, H.-J., Lee, H., Yoon, K.-S., & Cho, K. H. (2015). Optimizing low impact development (LID) for stormwater runoff treatment in urban area, Korea: Experimental and modeling approach. *Water Research*, *86*, 122–131.

Berndtsson, J. C. (2010). Green roof performance towards management of runoff water quantity and quality: A review. *Ecological Engineering*, *36*(4), 351–360.

Brattebo, B. O., & Booth, D. B. (2003). Long-term stormwater quantity and quality performance of permeable pavement systems. *Water Research*, *37*(18), 4369–4376.

Cacciuttolo, C., Garrido, F., Painenao, D., & Sotil, A. (2023). Evaluation of the use of permeable interlocking concrete pavement in Chile: Urban infrastructure solution for adaptation and mitigation against climate change. *Water*, *15*(24), 4219. https://doi.org/10.3390/w15244219

Chan, F. K. S., Griffiths, J. A., Higgitt, D., Xu, S., Zhu, F., Tang, Y.-T., Xu, Y., & Thorne, C. R. (2018). "Sponge City" in China—A breakthrough of planning and flood risk management in the urban context. *Land Use Policy*, *76*, 772–778. https://doi.org/10.1016/j.landusepol.2018.03.005

Chui, T. F. M., Liu, X., & Zhan, W. (2016). Assessing cost-effectiveness of specific LID practice designs in response to large storm events. *Journal of Hydrology*, *533*, 353–364.

Collins, K. A., Hunt, W. F., & Hathaway, J. M. (2008). Hydrologic comparison of four types of permeable pavement and standard asphalt in eastern North Carolina. *Journal of Hydrologic Engineering*, *13*(12), 1146–1157.

Dai, L., van Rijswick, H. F. M. W., Driessen, P. P. J., & Keessen, A. M. (2018). Governance of the Sponge City Programme in China with Wuhan as a case study. *International Journal of Water Resources Development*, *34*(4), 578–596. https://doi.org/10.1080/07900627.2017.1373637

Davis, A. P., Hunt, W. F., Traver, R. G., & Clar, M. (2009). Bioretention technology: Overview of current practice and future needs. *Journal of Environmental Engineering*, *135*(3), 109–117.

Dhakal, K. P., & Chevalier, L. R. (2017). Managing urban stormwater for urban sustainability: Barriers and policy solutions for green infrastructure application. *Journal of Environmental Management*, *203*, 171–181.

Dietz, M. E. (2007). Low impact development practices: A review of current research and recommendations for future directions. *Water, Air, & Soil Pollution*, *186*, 351–363. https://doi.org/10.1007/s11270-007-9484-z

Drake, J. A. P., Bradford, A., & Marsalek, J. (2013). Review of environmental performance of permeable pavement systems: State of the knowledge. *Water Quality Research Journal of Canada*, *48*(3), 203–222.

Eckart, K., McPhee, Z., & Bolisetti, T. (2017). Performance and implementation of low impact development – A review. *Science of the Total Environment*, *607–608*, 413–432.

Elliott, A. H., & Trowsdale, S. A. (2007). A review of models for low impact urban stormwater drainage. *Environmental Modelling & Software*, *22*(3), 394–405. https://doi.org/10.1016/j.envsoft.2005.12.005

Ferrans, P., Torres, M. N., Temprano, J., & Rodríguez Sánchez, J. P. (2022). Sustainable Urban Drainage System (SUDS) modeling supporting decision-making: A systematic quantitative review. *Science of the Total Environment*, *806*, 150447.

Fletcher, T. D., Shuster, W., Hunt, W. F., Ashley, R., Butler, D., Arthur, S., Trowsdale, S., Barraud, S., Semadeni-Davies, A., Bertrand-Krajewski, J.-L., Mikkelsen, P. S., Rivard, G., Uhl, M., Dagenais, D., & Viklander, M. (2015). SUDS, LID, BMPs, WSUD and more – The evolution and application of terminology surrounding urban drainage. *Urban Water Journal*, *12*(7), 525–542. https://doi.org/10.1080/1573062X.2014.916314

Fletcher, T. D., Andrieu, H., & Hamel, P. (2013). Understanding, management and modelling of urban hydrology and its consequences for receiving waters: A state of the art. *Advances in Water Resources*, *51*, 261–279.

Giacomoni, M. H., & Joseph, J. (2017). Multi-objective evolutionary optimization and Monte Carlo simulation for placement of low impact development in the catchment scale. *Journal of Water Resources Planning and Management*, *143*(9), 04017053.

Green, W. H., & Ampt, G. A. (1911). Studies on soil physics. *The Journal of Agricultural Science*, *4*(1), 1–24.

Griffiths, J., Chan, F. K. S., Shao, M., Zhu, F., & Higgitt, D. L. (2020). Interpretation and application of Sponge City guidelines in China. *Philosophical Transactions of the Royal Society A*, *378*(2168), 20190222. https://doi.org/10.1098/rsta.2019.0222

Hunt, W. F., Jarrett, A. R., Smith, J. T., & Sharkey, L. J. (2006). Evaluating bioretention hydrology and nutrient removal at three field sites in North Carolina. *Journal of Irrigation and Drainage Engineering*, *132*(6), 600–608.

Jiang, Y., Zevenbergen, C., & Ma, Y. (2018). Urban pluvial flooding and stormwater management: A contemporary review of China's challenges and "sponge cities" strategy. *Environmental Science & Policy*, *80*, 132–143. https://doi.org/10.1016/j.envsci.2017.11.016

Kabisch, N., Frantzeskaki, N., Pauleit, S., Naumann, S., Davis, M., Artmann, M., Haase, D., Knapp, S., Korn, H., Stadler, J., Zaunberger, K., & Bonn, A. (2016). Nature-based solutions to climate change mitigation and adaptation in urban areas: Perspectives on indicators, knowledge gaps, barriers, and opportunities for action. *Ecology and Society*, *21*(2), 39. https://doi.org/10.5751/ES-08373-210239

Kea, K., Dymond, R., & Campbell, W. (2016). An analysis of patterns and trends in United States stormwater utility systems. *Journal of the American Water Resources Association*, *52*(6), 1433–1449.

Kia, A., Wong, H. S., & Cheeseman, C. R. (2017). Clogging in permeable concrete: A review. *Journal of Environmental Management*, *193*, 221–233.

Kuruppu, U., Rahman, A., & Rahman, M. A. (2019). Permeable pavement as a stormwater best management practice: A review and discussion. *Environmental Earth Sciences*, *78*, 327.

Li, H., Ding, L., Ren, M., Li, C., & Wang, H. (2017). Sponge city construction in China: A survey of the challenges and opportunities. *Water*, *9*(9), 594. https://doi.org/10.3390/w9090594

Li, X.-J., Deng, J.-X., Xie, W.-J., Jim, C. Y., Wei, T.-B., Lai, J.-Y., & Liu, C.-C. (2022). Comprehensive benefit evaluation of pervious pavement based on China's sponge city concept. *Water*, *14*(9), 1500. https://doi.org/10.3390/w14091500

Lim, H. S., & Lu, X. X. (2016). Sustainable urban stormwater management in the tropics: An evaluation of Singapore's ABC Waters Program. *Journal of Hydrology*, *538*, 842–862.

Lin, Y., Liang, X., Xu, J., Song, Z., Lou, Y., & Yu, Y. (2024). Evaluation of the urban sponge stormwater regulation effectiveness based on SWMM: A case study of Wuhan, China. *Frontiers in Water*, *6*, 1406520. https://doi.org/10.3389/frwa.2024.1406520

Liu, W., Chen, W., & Peng, C. (2014). Assessing the effectiveness of green infrastructures on urban flooding reduction: A community scale study. *Ecological Modelling*, *291*, 6–14.

Liu, W., Chen, W., Feng, Q., Peng, C., & Kang, P. (2016). Cost-benefit analysis of green infrastructures on community stormwater reduction and utilization: A case of Beijing, China. *Environmental Management*, *58*(6), 1015–1026.

Lucke, T., & Beecham, S. (2011). Field investigation of clogging in a permeable pavement system. *Building Research & Information*, *39*(6), 603–615.

Mei, C., Liu, J., Wang, H., Yang, Z., Ding, X., & Shao, W. (2018). Integrated assessments of green infrastructure for flood mitigation to support robust decision-making for sponge city construction in an urbanized watershed. *Science of the Total Environment*, *639*, 1394–1407.

Mein, R. G., & Larson, C. L. (1973). Modeling infiltration during a steady rain. *Water Resources Research*, *9*(2), 384–394.

Moriasi, D. N., Arnold, J. G., Van Liew, M. W., Bingner, R. L., Harmel, R. D., & Veith, T. L. (2007). Model evaluation guidelines for systematic quantification of accuracy in watershed simulations. *Transactions of the ASABE*, *50*(3), 885–900.

Nash, J. E., & Sutcliffe, J. V. (1970). River flow forecasting through conceptual models part I — A discussion of principles. *Journal of Hydrology*, *10*(3), 282–290. https://doi.org/10.1016/0022-1694(70)90255-6

Nguyen, T. T., Ngo, H. H., Guo, W., Wang, X. C., Ren, N., Li, G., Ding, J., & Liang, H. (2019). Implementation of a specific urban water management – Sponge City. *Science of the Total Environment*, *652*, 147–162. https://doi.org/10.1016/j.scitotenv.2018.10.168

Palla, A., & Gnecco, I. (2015). Hydrologic modeling of Low Impact Development systems at the urban catchment scale. *Journal of Hydrology*, *528*, 361–368.

Philadelphia Water Department. (n.d.). *15 years of Green City, Clean Waters*. https://water.phila.gov/drops/15-years-of-green-city-clean-waters/ (accessed 13 October 2026).

Pochodyła, E., Glińska-Lewczuk, K., & Jaszczak, A. (2021). Blue-green infrastructure as a new trend and an effective tool for water management in urban areas. *Landscape Online*, *92*, 202192. https://doi.org/10.3097/LO.202192

Pochodyła-Ducka, E., Burandt, P., & Glińska-Lewczuk, K. (2025). GIS-based framework for assessing priority locations for blue-green infrastructure implementation in urban areas. *Ecological Indicators*, *176*, 113718. https://doi.org/10.1016/j.ecolind.2025.113718

PUB, Singapore's National Water Agency. (2018). *Active, Beautiful, Clean Waters (ABC Waters) design guidelines* (4th ed.). PUB.

Qi, Y., Chan, F. K. S., Thorne, C., O'Donnell, E., Quagliolo, C., Comino, E., Pezzoli, A., Li, L., Griffiths, J., Sang, Y., & Feng, M. (2020). Addressing challenges of urban water management in Chinese sponge cities via nature-based solutions. *Water*, *12*(10), 2788. https://doi.org/10.3390/w12102788

Qiao, X.-J., Kristoffersson, A., & Randrup, T. B. (2018). Challenges to implementing urban sustainable stormwater management from a governance perspective: A literature review. *Journal of Cleaner Production*, *196*, 943–952.

Randall, M., Sun, F., Zhang, Y., & Jensen, M. B. (2019). Evaluating Sponge City volume capture ratio at the catchment scale using SWMM. *Journal of Environmental Management*, *246*, 745–757. https://doi.org/10.1016/j.jenvman.2019.05.134

Rawls, W. J., Brakensiek, D. L., & Miller, N. (1983). Green-Ampt infiltration parameters from soils data. *Journal of Hydraulic Engineering*, *109*(1), 62–70.

Rossman, L. A., & Huber, W. C. (2016). *Storm Water Management Model reference manual, Volume I – Hydrology (revised)* (EPA/600/R-15/162A). U.S. Environmental Protection Agency, Office of Research and Development.

Rossman, L. A., & Simon, M. A. (2022). *Storm Water Management Model user's manual, version 5.2* (EPA/600/R-22/030). U.S. Environmental Protection Agency, Office of Research and Development.

Samai, B., Kebede, A. S., König, C. S., Martin-Moreta, P., & Kia, A. (2026). Process-based mechanisms and lifecycle mitigation of clogging in interlocking permeable pavements: Critical insights for sustainable urban drainage systems. *Water*, *18*(16), 2039. https://doi.org/10.3390/w18162039

Sansalone, J., Kuang, X., & Ranieri, V. (2008). Permeable pavement as a hydraulic and filtration interface for urban drainage. *Journal of Irrigation and Drainage Engineering*, *134*(5), 666–674.

Scholz, M., & Grabowiecki, P. (2007). Review of permeable pavement systems. *Building and Environment*, *42*(11), 3830–3836. https://doi.org/10.1016/j.buildenv.2006.11.016

Shuster, W. D., Bonta, J., Thurston, H., Warnemuende, E., & Smith, D. R. (2005). Impacts of impervious surface on watershed hydrology: A review. *Urban Water Journal*, *2*(4), 263–275.

Siriwardene, N. R., Deletic, A., & Fletcher, T. D. (2007). Clogging of stormwater gravel infiltration systems and filters: Insights from a laboratory study. *Water Research*, *41*(7), 1433–1440.

Sun, Y., Deng, L., Pan, S.-Y., Chiang, P.-C., Sable, S. S., & Shah, K. J. (2020). Integration of green and gray infrastructures for sponge city: Water and energy nexus. *Water-Energy Nexus*, *3*, 29–40. https://doi.org/10.1016/j.wen.2020.03.003

Sun, H., Wu, S., Dong, Q., Zhou, X., Yang, J., & Li, G. (2024). Research on runoff management of sponge cities under urban expansion. *Water*, *16*(15), 2103. https://doi.org/10.3390/w16152103

Thorne, C. R., Lawson, E. C., Ozawa, C., Hamlin, S. L., & Smith, L. A. (2018). Overcoming uncertainty and barriers to adoption of Blue-Green Infrastructure for urban flood risk management. *Journal of Flood Risk Management*, *11*, S960–S972.

Vineyard, D., Ingwersen, W. W., Hawkins, T. R., Xue, X., Demeke, B., & Shuster, W. (2015). Comparing green and grey infrastructure using life cycle cost and environmental impact: A rain garden case study in Cincinnati, OH. *Journal of the American Water Resources Association*, *51*(5), 1342–1360.

Walsh, C. J., Roy, A. H., Feminella, J. W., Cottingham, P. D., Groffman, P. M., & Morgan, R. P. (2005). The urban stream syndrome: Current knowledge and the search for a cure. *Journal of the North American Benthological Society*, *24*(3), 706–723.

Westra, S., Fowler, H. J., Evans, J. P., Alexander, L. V., Berg, P., Johnson, F., Kendon, E. J., Lenderink, G., & Roberts, N. M. (2014). Future changes to the intensity and frequency of short-duration extreme rainfall. *Reviews of Geophysics*, *52*(3), 522–555.

Winston, R. J., Dorsey, J. D., & Hunt, W. F. (2016). Quantifying volume reduction and peak flow mitigation for three bioretention cells in clay soils in northeast Ohio. *Science of the Total Environment*, *553*, 83–95.

Xia, J., Zhang, Y.-Y., Xiong, L.-H., He, S., Wang, L.-F., & Yu, Z.-B. (2017). Opportunities and challenges of the Sponge City construction related to urban water issues in China. *Science China Earth Sciences*, *60*(4), 652–658. https://doi.org/10.1007/s11430-016-0111-8

Yin, D., Chen, Y., Jia, H., Wang, Q., Chen, Z., Xu, C., Li, Q., Wang, W., Yang, Y., Fu, G., & Chen, A. S. (2021). Sponge city practice in China: A review of construction, assessment, operational and maintenance. *Journal of Cleaner Production*, *280*, 124963. https://doi.org/10.1016/j.jclepro.2020.124963

Yong, C. F., McCarthy, D. T., & Deletic, A. (2013). Predicting physical clogging of porous and permeable pavements. *Journal of Hydrology*, *481*, 48–55.

Zhang, K., & Chui, T. F. M. (2018). A comprehensive review of spatial allocation of LID-BMP-GI practices: Strategies and optimization tools. *Science of the Total Environment*, *621*, 915–929.

Zhang, K., & Chui, T. F. M. (2019). Linking hydrological and bioecological benefits of green infrastructures across spatial scales – A literature review. *Science of the Total Environment*, *646*, 1219–1231.

Zhou, Q. (2014). A review of sustainable urban drainage systems considering the climate change and urbanization impacts. *Water*, *6*(4), 976–992. https://doi.org/10.3390/w6040976

Zhou, Q., Leng, G., Su, J., & Ren, Y. (2019). Comparison of urbanization and climate change impacts on urban flood volumes: Importance of urban planning and drainage adaptation. *Science of the Total Environment*, *658*, 24–33.

Zhuang, J., Liang, Z., Lin, T., & De Guzman, F. (2007). *Theory and practice in the choice of social discount rate for cost-benefit analysis: A survey* (ERD Working Paper No. 94). Asian Development Bank. https://www.adb.org/publications/theory-and-practice-choice-social-discount-rate-cost-benefit-analysis-survey